IEEE Access
Multidisciplinary ⋮ Rapid Review ⋮ Open Access Journal

Received 28 February 2024, accepted 26 March 2024, date of publication 29 March 2024, date of current version 22 April 2024.

Digital Object Identifier 10.1109/ACCESS.2024.3383031

RESEARCH ARTICLE

Design of Hybrid Snake Optimizer Based Route Selection Approach for Unmanned Aerial Vehicles Communication

HEND KHALID ALKAHTANI[1], HANY MAHGOUB[2], FAIZ ABDULLAH ALOTAIBI[3], KAMAL M. OTHMAN[4], RANDA ALLAFI[5], AND AHMED S. SALAMA[6]

[1]Department of Information Systems, College of Computer and Information Sciences, Princess Nourah bint Abdulrahman University, P.O. Box 84428, Riyadh 11671, Saudi Arabia
[2]Department of Computer Science, College of Science and Art at Mahayil, King Khalid University, Abha 62529, Saudi Arabia
[3]Department of Information Science, College of Arts, King Saud University, P.O. Box 28095, Riyadh 11437, Saudi Arabia
[4]Department of Electrical Engineering, Umm Al-Qura University, Makkah 24382, Saudi Arabia
[5]Department of Computers and Information Technology, College of Sciences and Arts, Northern Border University, Arar 73213, Saudi Arabia
[6]Department of Electrical Engineering, Faculty of Engineering and Technology, Future University in Egypt, New Cairo 11845, Egypt

Corresponding author: Randa Allafi (Randa.allafi@nbu.edu.sa)

The authors extend their appreciation to the Deanship of Scientific Research at King Khalid University for funding this work through a large group Research Project under grant number (RGP2/96/44). Princess Nourah bint Abdulrahman University Researchers Supporting Project number (PNURSP2024R384), Princess Nourah bint Abdulrahman University, Riyadh, Saudi Arabia. Research Supporting Project number (RSPD2024R838), King Saud University, Riyadh, Saudi Arabia. The authors extend their appreciation to the Deanship of Scientific Research at Northern Border University, Arar, KSA for funding this research work through the project number NBU-FFR-2024-170-03. This study is partially funded by the Future University in Egypt (FUE).

ABSTRACT The effective usage of energy becomes crucial for the successful deployment and operation of unmanned aerial vehicles (UAVs) in different applications, such as surveillance, transportation, and communication networks. The increasing demand for UAVs in different industries such as agriculture, logistics, and emergency response has led to the development of more sophisticated and advanced UAVs. However, the limited onboard energy resource of UAVs poses a major problem for their long-term operation and endurance. In addition, artificial intelligence (AI) and machine learning (ML) could allow UAVs to make more informed and intelligent decisions regarding their operations, resulting in sustainable and more energy-efficient UAV deployment. This article designs a Hybrid Snake Optimizer-based Route Selection Approach for Unmanned Aerial Vehicles Communication (HSO-RSAUAVC) technique. The goal of the HSO-RSAUAVC technique is to explore and select optimal routes for UAV communication. In the presented HSO-RSAUAVC technique, the SO algorithm is integrated with Bernoulli Chaotic Mapping and Levy flight (LF) for enhanced performance. In addition, the HSO-RSAUAVC method derives a fitness function including residual energy (RE), distance, and UAV degree. By incorporating the HSO-RSAUAVC technique, we can dynamically adapt UAV paths to overcome obstacles, decrease communication interference, and optimize energy utilization. To validate the performance of the proposed model, a series of simulations were performed. The comparative result analysis illustrates the better performance of the HSO-RSAUAVC technique in improving the performance and reliability of UAV communication.

INDEX TERMS Unmanned aerial vehicles, routing, snake optimizer, energy efficiency, fitness function.

I. INTRODUCTION

Recently, with the fast growth of unmanned aerial vehicle (UAV) technology, UAVs have been extensively utilized in numerous domains [1]. Various kinds of UAVs can support people to accomplish some comparatively risky, impossible, and urgent tasks, like map reconstruction, ocean exploration, environmental analysis, aerial photography, and material distribution [2]. However, the existing UAVs are inadequately intelligent for performing difficult activities, and still major

The associate editor coordinating the review of this manuscript and approving it for publication was Cong Pu.

of them require people's real-time control [3]. A single UAV could only execute moderately easy tasks, nonetheless, the UAV set could effectively perform several laborious and complex tasks after acceptable task planning [4]. The task distribution issue is identical to the combinatorial optimizer decision issue for many UAVs. It is an integration method developed to satisfy UAV efficiency and limitations. The objective is to create a UAV that uses the smallest resources or acquires the maximal advantages with a shorter overall path [5]. The route planning issue includes planning a fight route from the initial to the endpoints in the restrained tasks space and creating the fitness function (FF) optimum. To resolve the task planning issue, several research works are carried out in a substantial number of studies [6]. The common task distribution technique comprises distributed methods (for instance, contract net auction method, decentralized Markov decision process, etc.), heuristic techniques (e.g., particle swarm optimization (PSO), Gas, ant colony approaches (ACOs), clustering methods, artificial bee colonies (ABC), and so on.) and optimization methods (for example, Hungarian method, graph theory, and branch definition algorithm) [7]. The common route planning approach comprises heuristic algorithms (A* algorithm, Dijkstra algorithm, Floyd algorithm, etc.), intelligent bionic approaches, and classical algorithms (for example, Voronoi diagram technique, artificial potential field algorithm, and so on) [8].

Route planning is a specific column of path planning with the goal of determining the path from an existing location to the target location [9]. The path must be smooth to align with the aircraft's flight characteristics [10]. Due to greater flexibility and mobility, UAVs have been more employed for performing variable and difficult tasks in the flight environment like post-disaster rescue and search and battlefield attack activities [11]. The investigation at home and foreign primarily highlights the route planning of the UAV in a fixed static environment [12]. Hence, the capability of UAVs to implement real-time maneuvering problem prevention and obtain dynamic environmental data becomes particularly significant [13].

This article designs a Hybrid Snake Optimizer-based Route Selection Approach for Unmanned Aerial Vehicles Communication (HSO-RSAUAVC) technique. In the presented HSO-RSAUAVC technique, the SO algorithm is integrated with Bernoulli Chaotic Mapping and Levy flight (LF) for enhanced performance. In addition, the HSO-RSAUAVC technique derives a fitness function (FF) including RE, distance, and UAV degree. By incorporating the HSO-RSAUAVC technique, we can dynamically adapt UAV paths to overcome obstacles, decrease communication interference, and optimize energy utilization. A series of experiments were performed to examine the performance of the HSO-RSAUAVC technique.

- Develop an HSO-RSAUAVC system intended to attain increased performance in route selection for UAV communication.
- Combine the SO technique with Bernoulli Chaotic Mapping and LF, exploiting the strengths of each to improve the effectiveness and efficiency of route selection in UAV communication.
- By integrating Bernoulli Chaotic Mapping and LF into the SO approach, the HSO-RSAUAVC system proposes to attain a higher solution with respect to route selection, and optimizing communication pathways.
- Presents a FF that comprises vital parameters namely RE, distance, and UAV degree. This holistic FF allows a widespread estimation of potential routes, assuming energy limitations, spatial requirements, and network connectivity.
- Assists dynamic adaptation of UAV paths. This adaptability allows UAVs to navigate around obstacles, decrease communication interference, and optimize energy consumption based on real-time conditions.

II. RELATED WORKS

Hilal et al. [14] developed a model called Group Teaching Optimization Algorithm with Deep Learning Enabled Smart Communication System (GTOADL-SCS) that follows two phases. Initially, a GTOA-based cluster system is utilized for organizing and electing Cluster Heads (CHs). Secondly, a FF includes 3 parameters of input. This model applied a pre-trained DenseNet_201 extractor along with gated recurrent unit (GRU) classifiers for classification. In [15], a real-world Three-Dimensional (3D) route planner used for UAV operation directed to its destiny via a hurdle-less route is presented. This presented route planner consists of a heuristic intelligence of $A\star$ model, but will not be needing frontier nodes for memory storage, unlike $A\star$. This planner depends on associative positions of recognized objects (hurdles) and decides clash-free routes. This route planner is less-weighted hence this swift guiding model for real-time needs. Alymani et al. [16] present a novel technique called Dispersal Foraging Strategy with Cuckoo Search Optimization-based Path Planning (DFSC-SOPP). In this work, the optimum route recognition for data transfer is achieved in UAV networking. Additionally, the method comprises optimum source distribution while identifying the network for optimum routes. However, this DFSCSO model can be constructed by combining the concept of DFS into the CSO model to eliminate the local optima issues.

In [17], a dual-route model for the swarm UAV network is constructed based on Random Network Coding (RNC). The initial route model uses the exclusive RNC aspect. Decoding can be performed on the primary packets as long as the UAV gathers enough generations. The subsequent route model additionally enhances the effectiveness in which every forwarding UAV just required to produce a novel generation instead of primary packet decoding. Manikandan and Sriramulu [18] suggested a new method known as Resilient UAV Path Optimization Algorithm (RUPOA) that gives an optimum route under safety outbreaks like

Man-in-the-Middle (MITM) and Denial-of-Service (DoS). For achieving a safe route plan in the UAV, and for mitigating safety outbreaks, a blockchain-assisted safety outcome is presented. For safety outbreak prevention, smart agreements are produced in which the equipment is listed with gasLimit. Wei and Xu [19] suggested a dispersed route strategy method depending on the dual decomposition UAV transmission chain. This method enhances the fundamental ant colony model from the path selector feature, pheromone update, and rollback policy considering the intrinsic restrictions of the ant colony model. For accomplishing the optimum model achievement, this study examines every ant colony model parameter deeply and attains the maximum parameter union.

Waqas et al. [20] introduced a path-finding model to mitigate the overhead encountered by reactive route models. This model not only addresses route overhead but also reduces energy consumption. To achieve this, the Time to Live (TTL) is altered to accommodate a huge node number in the search effort. This model also presented an alternate model for discrete application needs and associated the accomplishment with the modern expanding ring search (ERS) method. In [21], proposed a novel Parallel Cooperative Coevolutionary gray Wolf Optimizer (PCCGWO) technique, which enforces cooperative co-evolutionary perceptions for ensuring an effective divisor of the initial search space into multi-sub spacing. The decision variable vector decomposition into various sub-elements is accomplished and multi-swarm are formed from the primary populace. An effective equivalent master-slave method is suggested in the presented parameter-free PCCGWO.

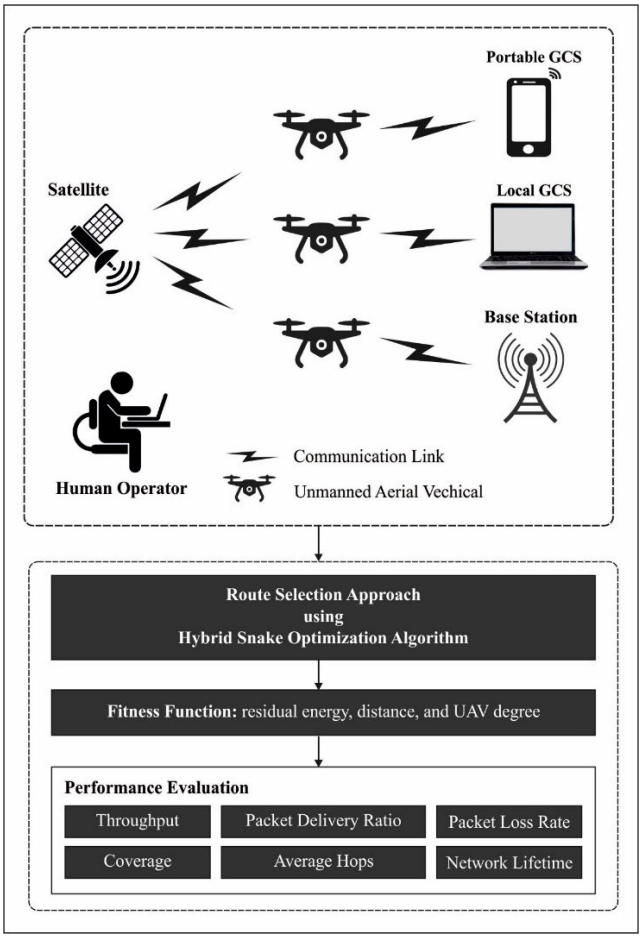

FIGURE 1. Overall flow of the HSO-RSAUAVC algorithm.

III. THE PROPOSED MODEL

In this article, a novel HSO-RSAUAVC method has been recognized for route selection in UAV communication networks. The purpose of the HSO-RSAUAVC method is to explore and select optimal routes for UAV communication. Fig. 1 portrays the entire flow of the HSO-RSAUAVC technique. The proposed method works through a refined incorporation of optimization methods to overcome the intrinsic challenges connected with UAV communication. By integrating the SO method with Bernoulli Chaotic Mapping and LF, the approach aims to accomplish greater route selection performance. The method includes the source of a comprehensive FF, such as residual energy, spatial distance, and UAV degree, enabling a holistic assessment of possible communication routes. The dynamic adaptation ability of the algorithm permits UAVs to autonomously modify their paths in real-time, which allows them to find around obstacles, decreasing communication interference, and optimizing energy consumption.

A. SYSTEM MODEL

The UAV can be modelled as a graph. All the nodes are constructed with omnidirectional antennae. Each node has a similar transmission power. Consider that nodes in the network have the subsequent characteristics:

1. All the nodes have a unique ID.
2. The nodes are considered as particles and move in two-dimensional space.
3. The nodes work in the half-duplex mode and it can be transmitting or receiving state.
4. The safe range of the node is a circular region and is less than its transmission range.
5. The geographic position data of all the nodes are exchanged with their neighbors.

B. MODELING OF HSO ALGORITHM

Snake optimizer (SO) is an optimization technique stimulated by the mating behaviors of the snake and constructing corresponding models to resolve it [22]. The mating procedure of snakes is largely confined by food quantity and temperature. The population initialization was produced by the standard distribution with the generation rules discussed as follows:

$$S_i = S_{\min} + rand_i \times (S_{max} - S_{\min}) \tag{1}$$

In Eq. (1), S_i signifies the location of the population individual at the t^{th} time, $rand_i$ represents the random integer

within [0, 1] at the t^{th} time, and S_{max} and S_{min} symbolize the maximum and minimum boundaries of the population.

The distribution of amount of individual females and males according to gender begins after attaining the initial population. Generally, the amount of female and male individuals are equal. Thus, the number of females and males is evaluated as follows:

$$N_m = N_f = \frac{N_{all}}{2} \tag{2}$$

In Eq. (2), N_{all} refers to the overall population size, N_m and N_f correspondingly show the amount of males and females.

In SO, food quantity and temperature are dual crucial causes that define snake mating, and temperature and food quantity are determined as follows:

$$Temp = e^{-t/T} \tag{3}$$

$$FQ = c_1 \times e^{(t-T)/T} \tag{4}$$

From the expression, t shows the existing iteration count, T specifies the overall amount of iterations, and c_1 denotes the fixed constant of 0.5.

In the exploration stage, if $FQ < 0.25$, then the snake finds food by choosing and updating the location randomly.

$$\begin{aligned} S_i^m(t+1) &= S_{rand}^m(t) \oplus c_2 \times e^{-\frac{f_{ransd}^m}{f_i^m}} \times S_i \\ &= \begin{cases} S_{rand}^m(t) + c_2 \times e^{-\frac{f_{rand}^m}{f_i^m}} \times S_i \\ S_{rand}^m(t) - c_2 \times e^{-\frac{f_{rand}^m}{f_i^m}} \times S_i \end{cases} \end{aligned} \tag{5}$$

$$\begin{aligned} S_i^f(t+1) &= S_{rand}^f(t) \oplus c_2 \times e^{-\frac{f_{rand}^f}{f_i^f}} \times S_i \\ &= \begin{cases} S_{rand}^f(t) + c_2 \times e^{-\frac{f_{rand}}{f_i^f}} \times S_i \\ S_{rand}^f(t) - c_2 \times e^{-\frac{f_{rand}}{f_i^f}} \times S_i \end{cases} \end{aligned} \tag{6}$$

where S_i^f indicates the location of the females at the t^{th} time, S_i^m signifies the location of males at *the* t^{th} time and S_{rand}^m shows the random location of the male snake. f_{rand}^m denotes the fitness of the male snake S_{rand}^m, and f_i^m refers to the individual fitness of the males at t^{th} time. and S_{rond}^f indicates the random location of the female snake. f_{rand}^f shows the individual fitness of t^{th} female snake S_{rand}^f, c_2 denotes a constant set to 0.05 and $\oplus$ indicates the sign direction operator.

In the exploration stage, if $FQ > 0.25$ and $Temp > 0.6$, then the snake eats only the food and doesn't go into the mating procedure.

$$\begin{aligned} &S_i^{m,f}(t+1) \\ &= S_{food} \oplus c_3 \times Temp \times rand_i \times \left(S_{food} - S_i^{m,f}(t)\right) \\ &= \begin{cases} S_{food} + c_3 \times Temp \times rand_i \times \left(S_{food} - S_i^{m,f}(t)\right) \\ S_{food} - c_3 \times Temp \times rand_i \times \left(S_{food} - S_i^{m,f}(t)\right) \end{cases} \end{aligned} \tag{7}$$

where c_3 shows the fixed constant of 2, $S_i^{m,f}$ denotes the individual location of males or females, and S_{food} represents the location of the optimum individual.

If $FQ > 0.25$ and $Temp \leq 0.6$, then the snake enters into the mating part, and there is an option of competition among individual females and males since the individual male or female wants to complete mating with the superior heterosexual. First, the charming individual chooses the mating partner, fighting and mating modes are the two mating parts of SO, and the fighting mode can be denoted as follows.

$$\begin{aligned} S_i^m(t+1) &= S_i^m(t) + c_3 \times e^{-f_{best}/f_i} \times rand_j \\ &\quad \times \left(FQ \times S_{best}^f - S_i^m(t)\right) \end{aligned} \tag{8}$$

$$\begin{aligned} S_i^f(t+1) &= S_i^f(t) + c_3 \times e^{-f_{best}^m/f_i} \times rand_i \\ &\quad \times \left(FQ \times S_{best}^m - S_i^f(t)\right) \end{aligned} \tag{9}$$

where S_i^f represents the location of the female snake at i^{th} generation, f_{best}^f, and f_{best}^m imply the optimum fitness of the individual female and male snakes during the fight mode, S_i^m indicates the location of the male snake at i^{th} generation, S_{best}^f shows the optimum location of the individual female snake, S_{best}^m means the optimum location of the individual male snake, and f_i signifies individual fitness. Fig. 2 represents the flowchart of the SO algorithm.

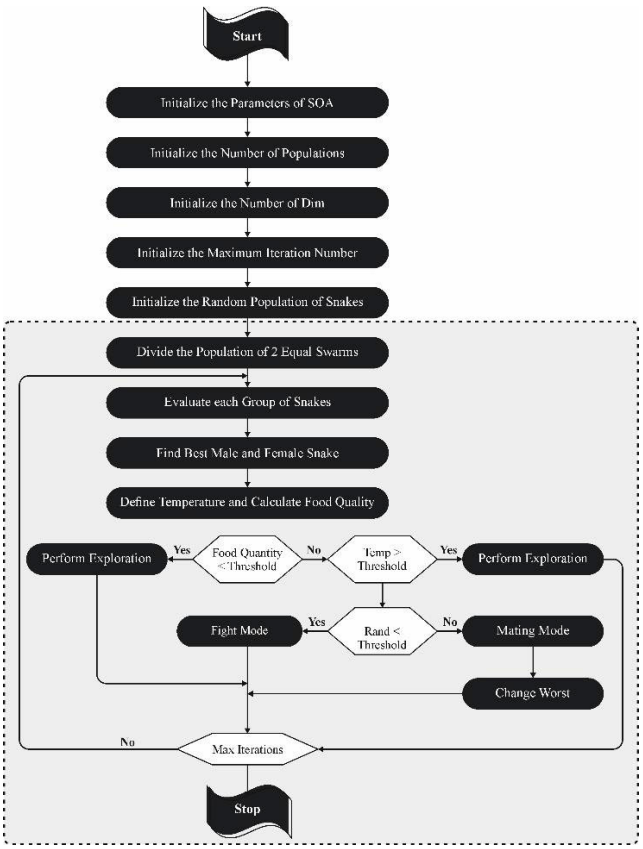

FIGURE 2. Flowchart of SO algorithm.

The mating process can be formulated using Eqs. (10) & (11).

$$S_i^m(t+1) = S_i^m(t) + c_3 \times e^{-m_i^f/f_i^m} \times rand_i \times (FQ \times S_i^f(t) - S_i^m(t)) \quad (10)$$

$$S_i^f(t+1) = S_i^f(t) + c_3 \times e^{-m_i^f/fi} \times rand_i \times (FQ \times S_i^m(t) - S_i^f(t)) \quad (11)$$

where m_i^m and m_i^{fs} symbolize the fitness of i^{th} individuals during the mating pattern. S_i^m and S_i^f denote the location of the i^{th} individuals in the male and female snakes.

After finishing the mating, the female snake will lay their eggs to attain a novel snake and in the original population, it replaces the worst individual female or male, based on the gender of novel snakes, correspondingly.

$$S_{worst}^m = S_{\min} + rand_j \times (S_{\max} - S_{\min}) \quad (12)$$

$$S_{worst}^f = S_{\min} + rand_j \times (S_{\max} - S_{\min}) \quad (13)$$

In Eq. (13), S_{worst}^m and S_{worst}^f refers to the worst individuals amongst individual males and females.

In the presented HSO-RSAUAVC technique, the SO algorithm is integrated with Bernoulli Chaotic Mapping and LF for enhanced performance [23]. The solution accurateness and union rate of the technique were influenced by the quality of population initialization. Improving the searching ability of the model was accomplished by the high-quality early population. The sequence of chaotic mapping lacks the features of orderliness and ergodicity, which enables it to expedite convergence speed, improve the distribution diversity of the population, and yield a high-quality early population. The population initialization made by Bernoulli chaotic mapping is given in the following expression:

$$Z_i^d = \begin{cases} Z_i^d/(1-\theta), & 0 < Z_i^d < 1-\theta \\ (Z_i^d - 1+\theta)/\lambda, & 1-\theta < Z_i^d < 1 \end{cases} \quad (14)$$

In Eq. (14), λ indicates a constant; i denotes the amount of particles; d shows the dimension; and θ takes the value of 0.5.

Depending on the Bernoulli chaotic sequence, the initial population can be produced after attaining an initial value of Bernoulli chaotic mapping using Eq. (17) as follows:

$$C_i^d = C_{\min}^d + Z_i^d \left(C_{\max}^d - C_{\min}^d\right) \quad (15)$$

The application of the random walking characteristics of LF has found increased use in optimization algorithms, comprising the GWO and PSO algorithms that could enhance the capability of the model to boost algorithmic performance, escape local optima, and ultimately improve the diversity of search spaces. Generally, the step size of LF is a uniformly distributed random value, and its step size can be given as follows.

$$s = \frac{\mu}{|v|^{\frac{1}{\beta}}} \quad (16)$$

In Eq. (16), $\mu = N\left(0, \delta_\mu^2\right)$ and $v = N\left(0, \delta_v^2\right)$ are uniform random distribution; β take the value of 1.5 =; and the formula of δ_μ and δ_v are given as follows:

$$\delta_\mu = \left(\frac{\Gamma(1+\beta) \cdot sin\left(\pi \cdot \frac{\beta}{2}\right)}{\beta \cdot \Gamma\left(\frac{1+\beta}{2}\right) \cdot 2^{\frac{\beta-1}{2}}}\right)^{\frac{1}{\beta}} \quad (17)$$

$$\delta_v = 1 \quad (18)$$

The path of LF satisfies its random walking properties to guarantee that the model hunts in the wide-ranging space and employs it to the concentration update; hence, the equation can be given as follows:

$$C = C_{eq} + \left(C - C_{eq}\right) \cdot F \cdot s \cdot 0.01 + \frac{G}{\lambda V}(1-F) \quad (19)$$

C. ROUTE SELECTION PROCESS

The HSO-RSAUAVC method derives an FF including RE, distance, and UAV degree. The derived probable energy function is dependent upon the provided features.

RE level: The major objective is that the relay node (RN) to the upcoming hop node is dependent upon the RE of the later hop node. The RN node elects the future hop RN on the potential hop node, but it can be superior RE.

Objective1: Maximize

$$g_1 = \sum_{j=1}^{m} NextHop\left(E_R\left(CHj\right)\right) \quad (20)$$

Distance to the base station (BS): Every RN to the next hop node is dependent upon the distance to upcoming hop nodes and the distance contained node to sink.

Objective2: Minimize

$$g_2 = \sum_{j=1}^{m} dis(CH_j, NextHop\left(CH_j\right) + dis\left(Nexthop\left(CH_j\right), BS\right) \quad (21)$$

Node degree: The main drive of every RN to the next hop node is dependent upon node degree. The RN is pointed out to the upcoming hop node exploiting a lesser node degree.

Objective3: Minimize

$$g_3 = \sum_{j=1}^{m} Node\ degree\ of\ Next\ Hop\left(CHj\right) \quad (22)$$

It could be the weighted summation method to optimizer method after the drives are inclined to RN other.

Minimize

$$Potential\ energy\ function = \beta_1 \times \frac{1}{g_1} + \beta_2 \times g_2 + \beta_3 \times g_3 \quad (23)$$

In which, $0 < \beta_1, \beta_2, \beta_3 < 1$ *and* $0 < g_1, g_2, g_3 < 1$

Then, the HSO-RSAUAVC approach is to elect the next hop node exploiting the superior energy function. Next, the RN transmits the combined data in its member to BS with the elected optimum path.

IV. RESULTS AND DISCUSSION

The proposed method was examined in the field with BS, and UAVs positioned employing the Poisson distribution area of 50×50 m^2. The initial power of IoE-objects can be measured at 100 J, and for UAVs, it is deliberated that the power is higher than the requirement of all UAVs. For the accessibility of the simulations, the initial power of UAVs is 2000 J. Segments differ between 3 m and 5 for every BS. The IoE-objects in Ue-IoE vary among 100 and 350. With the help of the conventional technique, the power consumption for a UAV is 0.5 J. The UAV frequency is in the middle of 5 and 10 m and the output voltage of the UAV remains 500 m.

In this part, the performance outcome of the HSO-RSAUAVC approach was tested below varying aspects. Table 1 and Fig. 3 inspect an overall throughput (THRO) result of the HSO-RSAUAVC system with different approaches [16]. The outcome shows that the HSO-RSAUAVC system achieves enhanced performance. With 5% of energy consumption (ECOM), the HSO-RSAUAVC technique offers higher THRO of 68bytes/s but the TRU-AVS, UAVeWSN, ORPFANET, ESROSRP, and DFSCSOPP algorithms obtain decreased ECOM values of 4bytes/s, 10bytes/s, 20bytes/s, 33bytes/s, and 50bytes/s respectively. Meanwhile, with 100% of ECOM, the HSO-RSAUAVC approach attains enhanced THRO of 212bytes/s while the TRUAVS, UAVeWSN, ORPFANET, ESROSRP, and DFSCSOPP systems obtain decreased ECOM values of 92bytes/s, 115bytes/s, 122bytes/s, 184bytes/s, and 197bytes/s correspondingly.

TABLE 1. THRO outcome of HSO-RSAUAVC algorithm with other methodologies under varying ECOM.

Throughput (bytes/sec)						
Energy Consumption (%)	TRU AVS	UAVe WSN	ORPF ANET	ESRO SRP	DFSC SOPP	HSO-RSAU AVC
5	4	10	20	33	50	68
10	6	13	19	38	57	73
15	8	12	25	43	74	89
20	12	18	27	63	92	109
25	11	22	30	87	107	124
30	15	27	36	114	128	144
35	18	30	40	127	147	165
40	24	36	49	139	158	173
45	25	44	58	145	167	185
50	34	52	65	149	178	194
55	39	56	75	151	182	200
60	46	62	84	151	187	203
65	51	73	88	154	191	208
70	56	80	98	158	195	212
75	63	86	106	163	197	212
80	68	92	113	171	197	214
85	78	99	115	179	197	213
90	85	104	118	181	197	212
95	88	113	122	184	197	214
100	92	115	122	184	197	212

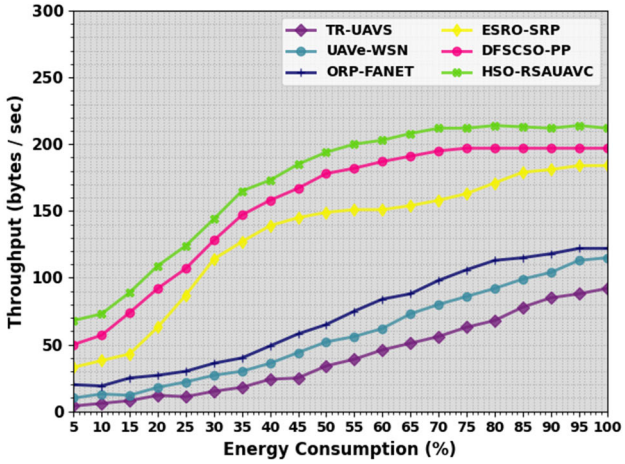

FIGURE 3. THRO outcome of HSO-RSAUAVC algorithm under varying ECOM.

TABLE 2. PDR outcome of HSO-RSAUAVC algorithm with other methodologies under varying ECOM.

Packet Delivery Ratio (%)						
Energy Consumption (%)	TRU AVS	UAVe WSN	ORPF ANET	ESRO SRP	DFSC SOPP	HSO-RSAU AVC
5	42.98	43.42	48.53	65.59	74.02	80.96
10	42.43	44.44	52.16	67.21	76.89	83.12
15	43.48	48.26	54.91	68.46	80.03	88.16
20	44.56	50.19	56.50	70.75	81.50	89.51
25	46.16	52.25	57.41	73.12	82.74	89.38
30	47.10	53.82	59.53	75.35	84.21	92.77
35	48.12	54.62	61.18	75.99	85.25	91.82
40	50.04	56.10	63.44	76.29	85.54	91.21
45	50.46	55.93	64.42	76.67	86.53	93.92
50	51.97	55.83	65.64	76.90	88.55	95.80
55	53.07	57.18	66.65	79.53	89.36	96.88
60	53.66	58.55	67.18	79.95	90.36	95.93
65	53.55	60.99	69.07	80.57	90.80	97.91
70	54.30	63.14	70.26	82.85	91.15	96.68
75	56.38	63.99	71.23	86.00	92.21	95.94
80	58.65	65.81	73.86	84.69	92.92	96.54
85	59.21	66.70	74.27	85.66	94.06	97.59
90	60.14	67.36	74.36	85.68	94.06	97.79
95	62.77	68.74	75.01	87.45	94.45	98.22
100	63.29	68.75	75.87	87.24	94.76	98.32

Table 2 and Fig. 4 demonstrate an overall packet delivery ratio (PDR) outcome of the HSO-RSAUAVC algorithm with different systems. The outcome values depicted that the HSO-RSAUAVC approach attains enhanced performance. With 5% of ECOM, the HSO-RSAUAVC system offers a greater PDR of 80.96% whereas the TRUAVS, UAVeWSN, ORPFANET, ESROSRP, and DFSCSOPP models obtain decreased ECOM values of 42.98%, 43.42%,

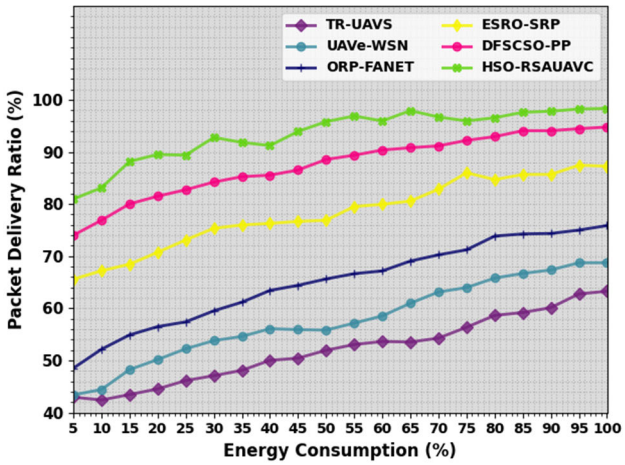

FIGURE 4. PDR outcome of HSO-RSAUAVC algorithm under varying ECOM.

TABLE 3. AHOPS outcome of HSO-RSAUAVC algorithm with other methodologies under varying ECOM.

Average HOPS (%)						
Energy Consumption (%)	TRUAVS	UAVeWSN	ORPFANET	ESROSRP	DFSCSOPP	HSO-RSAUAVC
5	2.49	4.23	6.19	10.59	14.22	17.75
10	2.87	4.94	7.38	10.43	15.72	19.28
15	2.59	5.10	7.71	11.32	17.59	21.00
20	2.76	5.67	8.05	12.81	17.93	21.45
25	2.99	5.84	9.08	15.11	19.00	22.68
30	3.19	6.47	9.76	16.68	19.90	23.43
35	3.65	6.61	10.36	17.62	21.60	25.16
40	4.28	6.92	11.10	17.68	21.75	25.26
45	4.58	7.16	12.18	18.45	22.21	25.82
50	4.56	7.43	12.29	18.88	22.49	25.92
55	4.98	7.63	12.45	19.42	22.88	26.37
60	5.49	8.20	13.45	20.99	23.89	27.14
65	5.07	8.31	13.16	21.45	24.42	27.99
70	6.14	8.93	13.29	21.42	24.46	27.69
75	6.38	9.01	15.14	22.48	25.03	28.46
80	6.81	9.57	17.98	22.61	25.12	28.64
85	7.70	10.19	19.22	23.01	25.67	29.20
90	7.97	9.82	20.02	23.16	25.79	29.36
95	7.99	10.04	20.57	24.46	25.91	29.13
100	7.71	10.53	20.60	24.99	25.83	29.37

48.53%, 65.59%, and 74.02% correspondingly. In the meantime, with 100% of ECOM, the HSO-RSAUAVC technique offers superior PDR of 98.32% but the TRUAVS, UAVeWSN, ORPFANET, ESROSRP, and DFSCSOPP approaches obtain lesser ECOM values of 63.29%, 68.75%, 75.87%, 87.24%, and 94.76% correspondingly.

Table 3 and Fig. 5 examine the overall average hops (AHOPS) analysis of the HSO-RSAUAVC approach with different methods. The simulation outcome exhibited that the HSO-RSAUAVC approach reaches improved performance.

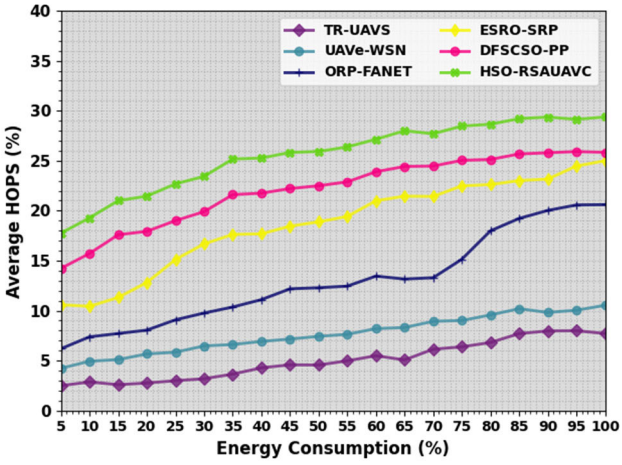

FIGURE 5. AHOPS outcome of HSO-RSAUAVC algorithm under varying ECOM.

TABLE 4. Coverage outcome of the HSO-RSAUAVC algorithm with other methodologies under varying ECOM.

Coverage (%)						
Energy Consumption (%)	TRUAVS	UAVeWSN	ORPFANET	ESROSRP	DFSCSOPP	HSO-RSAUAVC
5	61.43	73.22	79.59	95.05	97.27	99.13
10	61.37	73.84	80.31	96.02	97.52	98.3
15	61.89	73.65	79.59	94.48	97.72	98.16
20	59.94	72.44	76.2	93.44	97.05	98.13
25	57.52	70.18	73.34	89.41	95.98	98.4
30	53.59	66.41	69.48	87.33	94.44	96.19
35	48.12	60.26	64.66	85.59	90.77	92.18
40	43.24	55.09	61.75	83.1	86.56	89.21
45	39.94	50.28	57.21	77.68	80.56	81.72
50	35.11	46.17	53.79	74.5	76.21	79.02
55	33.4	42.16	49.72	66.77	73.11	75.14
60	29.07	39.83	46.31	63.43	71.82	73.67
65	26.86	35.12	42.89	62.72	69.5	72.09
70	23.17	33.6	38.78	62.26	70.12	71.12
75	20.64	30.66	36	60.86	65.78	68.2
80	18.9	26.01	34.88	53.07	62.74	63.78
85	14.31	21.3	32.07	51.09	61.35	62.45
90	12.03	17.8	29.38	47.71	59.32	60.81
95	7.5	15.64	27.69	48	56.61	58.19
100	6.43	13.57	22.62	47.31	53.23	54.67

With 5% of ECOM, the HSO-RSAUAVC system attains maximal AHOPS of 17.75% but the TRUAVS, UAVeWSN, ORPFANET, ESROSRP, and DFSCSOPP approaches gain lesser ECOM values of 2.49%, 4.23%, 6.19%, 10.5% and 14.2% respectively. Afterwards, with 100% of ECOM, the HSO-RSAUAVC algorithm offers improved AHOPS of 98.32% whereas the TRUAVS, UAVeWSN, ORPFANET, ESROSRP, and DFSCSOPP systems obtain decreased

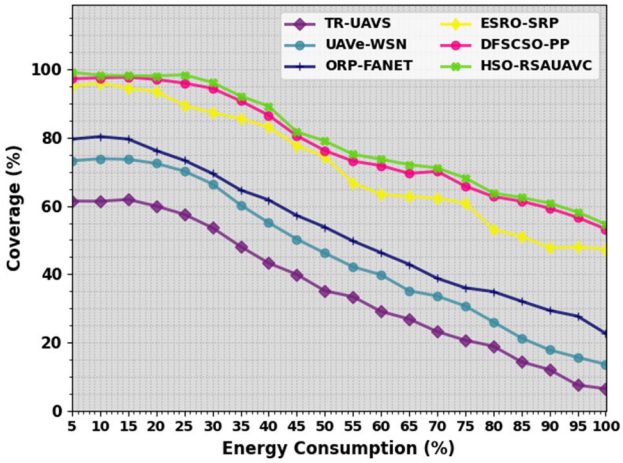

FIGURE 6. Coverage outcome of HSO-RSAUAVC algorithm under varying ECOM.

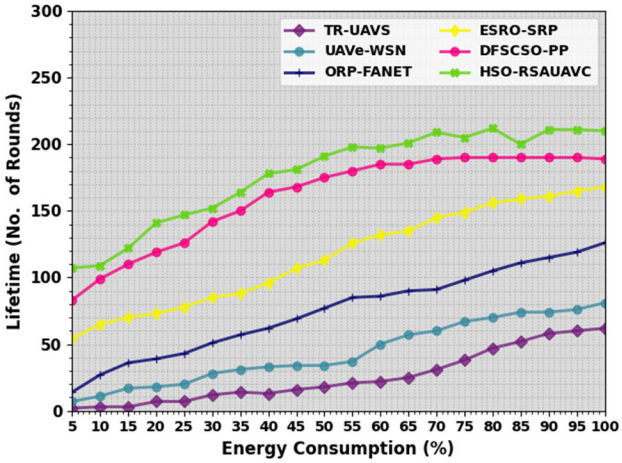

FIGURE 7. Lifetime outcome of HSO-RSAUAVC algorithm under varying ECOM.

TABLE 5. Lifetime outcome of HSO-RSAUAVC algorithm with other methodologies under varying ECOM.

Lifetime (No. of Rounds)						
Energy Consumption (%)	TRUAVS	UAVeWSN	ORPFANET	ESROSRP	DFSCSOPP	HSO-RSAUAVC
5	2	7	14	54	83	107
10	3	11	27	65	99	109
15	3	17	36	70	110	122
20	7	18	39	73	119	141
25	7	20	43	78	126	147
30	12	28	51	85	142	152
35	14	31	57	88	150	164
40	13	33	62	96	164	178
45	16	34	69	107	168	181
50	18	34	77	113	175	191
55	21	37	85	126	180	198
60	22	50	86	132	185	197
65	25	57	90	135	185	201
70	31	60	91	145	189	209
75	38	67	98	149	190	205
80	47	70	105	156	190	212
85	52	74	111	159	190	200
90	58	74	115	161	190	211
95	60	76	119	165	190	211
100	62	81	126	168	189	210

ECOM values of 29.37%, 7.71%, 10.5%, 20.6%, 24.9% and 25.8% correspondingly.

Table 4 and Fig. 6 depict an overall coverage (COV) outcome of the HSO-RSAUAVC algorithm with different approaches. The outcome exhibited that the HSO-RSAUAVC approach gains better outcomes. With 5% of ECOM, the HSO-RSAUAVC algorithm offers a maximum COV of 99.13% where the TRUAVS, UAVeWSN, ORPFANET, ESROSRP, and DFSCSOPP approaches obtain minimal ECOM values of 61.43%, 73.22%, 79.59%, 95.05% and 97.27% correspondingly. Likewise, with 100% of ECOM, the HSO-RSAUAVC approach achieves a higher COV of 54.67% but the TRUAVS, UAVeWSN, ORPFANET, ESROSRP, and DFSCSOPP methods obtain decreased ECOM values of 6.43%, 13.5%, 22.6%, 47.3% and 53.2% correspondingly.

Table 5 and Fig. 7 depict an overall lifetime (LFT) examination of the HSO-RSAUAVC algorithm with different approaches. The result demonstrated that the HSO-RSAUAVC system achieves higher performance. With 5% of ECOM, the HSO-RSAUAVC system obtains enhanced LFT of 107 rounds but the TRUAVS, UAVeWSN, ORPFANET, ESROSRP, and DFSCSOPP models obtain decreased ECOM values of 2, 7, 14, 54, and 83 rounds correspondingly. Afterwards, with 100% of ECOM, the HSO-RSAUAVC approach obtains maximal LFT of 210 rounds whereas the TRUAVS, UAVeWSN, ORPFANET, ESROSRP, and DFSCSOPP system attain lesser ECOM values of 62, 81, 126, 168, and 189 rounds correspondingly.

These results ensured that the HSO-RSAUAVC technique accomplishes enhanced performance over other models.

V. CONCLUSION

In this article, a new HSO-RSAUAVC technique has been recognized for route selection in UAV communication networks. The purpose of the HSO-RSAUAVC technique is to explore and select optimal routes for UAV communication. In the presented HSO-RSAUAVC technique, the SO algorithm is integrated with Bernoulli Chaotic Mapping and LF for enhanced performance. In addition, the HSO-RSAUAVC method derives an FF including RE, distance, and UAV degree. By incorporating the HSO-RSAUAVC technique, we can dynamically adapt UAV paths to overcome obstacles, decrease communication interference, and optimize energy utilization. An experimental evaluation process is performed to examine the performance of the HSO-RSAUAVC technique. The obtained results demonstrate the significance of improving the performance and reliability of UAV communication. In terms of real-time applications, the HSO-RSAUAVC algorithm is possible in monitoring and surveillance, disaster response, precision agriculture, and other mission-critical processes. The method's capability to

adjust UAV paths on the fly can offer improved reliability and efficiency in communication networks, making it competent for situations where early and accurate data will be crucial.

For future work, research workers will explore the adaptability and scalability of the HSO-RSAUAVC method to adapt to a huge number of UAVs in collaborative missions. This could involve analyzing the model's robustness in conditions with dynamic environmental circumstances and changing mission requirements. Moreover, efforts are directed toward real-time execution and testing of the HSO-RSAUAVC algorithm in real-time UAV applications. This comprises incorporation with actual UAV platforms for measuring its effectiveness in real-time communication settings. Future work aims to explore the integration of emerging technologies such as 5G and edge computing to enhance real-time decision-making and optimize energy utilization. Besides, upcoming work can examine the scalability of the HSO-RSAUAVC technique for large-scale UAV networks and investigate its applicability in various operational scenarios, including disaster response and precision agriculture.

ACKNOWLEDGMENT

The authors extend their appreciation to the Deanship of Scientific Research at King Khalid University for funding this work through a large group Research Project under grant number (RGP2/96/44). Princess Nourah bint Abdulrahman University Researchers Supporting Project number (PNURSP2024R384), Princess Nourah bint Abdulrahman University, Riyadh, Saudi Arabia. Research Supporting Project number (RSPD2024R838), King Saud University, Riyadh, Saudi Arabia. The authors extend their appreciation to the Deanship of Scientific Research at Northern Border University, Arar, KSA for funding this research work through the project number NBU-FFR-2024-170-03. This study is partially funded by the Future University in Egypt (FUE).

REFERENCES

[1] M. Ali, K. N. Qureshi, T. Newe, K. Aman, A. O. Ibrahim, M. Almujaly, and W. Nagmeldin, "Decision-based routing for unmanned aerial vehicles and Internet of Things networks," *Appl. Sci.*, vol. 13, no. 4, p. 2131, Feb. 2023.

[2] S. K. Jha, S. Prakash, R. S. Rathore, M. Mahmud, O. Kaiwartya, and J. Lloret, "Quality-of-service-centric design and analysis of unmanned aerial vehicles," *Sensors*, vol. 22, no. 15, p. 5477, Jul. 2022.

[3] S. B. Son and D. H. Kim, "Searching for scalable networks in unmanned aerial vehicle infrastructure using spatio-attack course-of-action," *Drones*, vol. 7, no. 4, p. 249, Apr. 2023.

[4] X. Qiu, L. Xu, P. Wang, Y. Yang, and Z. Liao, "A data-driven packet routing algorithm for an unmanned aerial vehicle swarm: A multi-agent reinforcement learning approach," *IEEE Wireless Commun. Lett.*, vol. 11, no. 10, pp. 2160–2164, Oct. 2022.

[5] X. Yu, C. Li, and G. G. Yen, "A knee-guided differential evolution algorithm for unmanned aerial vehicle path planning in disaster management," *Appl. Soft Comput.*, vol. 98, Jan. 2021, Art. no. 106857.

[6] B. Ma, Z. Liu, Q. Dang, W. Zhao, J. Wang, Y. Cheng, and Z. Yuan, "Deep reinforcement learning of UAV tracking control under wind disturbances environments," *IEEE Trans. Instrum. Meas.*, vol. 72, pp. 1–13, 2023.

[7] B. Ma, Z. Liu, W. Zhao, J. Yuan, H. Long, X. Wang, and Z. Yuan, "Target tracking control of UAV through deep reinforcement learning," *IEEE Trans. Intell. Transp. Syst.*, pp. 1–18, 2023.

[8] B. Ma, Z. Liu, F. Jiang, W. Zhao, Q. Dang, X. Wang, J. Zhang, and L. Wang, "Reinforcement learning based UAV formation control in GPS-denied environment," *Chin. J. Aeronaut.*, vol. 36, no. 11, pp. 281–296, Nov. 2023.

[9] J. Li, S. Li, and C. Xue, "Resource optimization for multi-unmanned aerial vehicle formation communication based on an improved deep Q-network," *Sensors*, vol. 23, no. 5, p. 2667, Feb. 2023.

[10] M. T. R. Khan, M. Muhammad Saad, Y. Ru, J. Seo, and D. Kim, "Aspects of unmanned aerial vehicles path planning: Overview and applications," *Int. J. Commun. Syst.*, vol. 34, no. 10, p. e4827, Jul. 2021.

[11] X. Meng, X. Zhu, and J. Zhao, "Obstacle avoidance path planning using the elite ant colony algorithm for parameter optimization of unmanned aerial vehicles," *Arabian J. Sci. Eng.*, vol. 48, no. 2, pp. 2261–2275, Feb. 2023.

[12] N. A. Kyriakakis, M. Marinaki, N. Matsatsinis, and Y. Marinakis, "A cumulative unmanned aerial vehicle routing problem approach for humanitarian coverage path planning," *Eur. J. Oper. Res.*, vol. 300, no. 3, pp. 992–1004, Aug. 2022.

[13] S. Huang, F. Liao, and R. S. H. Teo, "Fault tolerant control of quadrotor based on sensor fault diagnosis and recovery information," *Machines*, vol. 10, no. 11, p. 1088, Nov. 2022.

[14] A. M. Hilal, J. S. Alzahrani, D. H. Elkamchouchi, H. Dalia, M. M. Eltahir, A. S. Almasoud, A. Motwakel, A. S. Zamani, and I. Yaseen, "Optimal deep learning enabled communication system for unmanned aerial vehicles," *Comput. Syst. Sci.*, vol. 45, no. 1, pp. 955–969, 2023.

[15] A. Tullu, B. Endale, A. Wondosen, and H.-Y. Hwang, "Machine learning approach to real-time 3D path planning for autonomous navigation of unmanned aerial vehicle," *Appl. Sci.*, vol. 11, no. 10, p. 4706, May 2021.

[16] M. Alymani, H. Alsolai, M. Maashi, A. Alhebri, H. Alshahrani, F. N. Al-Wesabi, A. Mohamed, and M. A. Hamza, "Dispersal foraging strategy with cuckoo search optimization based path planning in unmanned aerial vehicle networks," *IEEE Access*, vol. 11, pp. 31365–31372, 2023.

[17] H. Song, L. Liu, S. M. Pudlewski, and E. S. Bentley, "Random network coding enabled routing protocol in unmanned aerial vehicle networks," *IEEE Trans. Wireless Commun.*, vol. 19, no. 12, pp. 8382–8395, Dec. 2020.

[18] K. Manikandan and R. Sriramulu, "Optimized path planning strategy to enhance security under swarm of unmanned aerial vehicles," *Drones*, vol. 6, no. 11, p. 336, Nov. 2022.

[19] X. Wei and J. Xu, "Distributed path planning of unmanned aerial vehicle communication chain based on dual decomposition," *Wireless Commun. Mobile Comput.*, pp. 1–12, Jun. 2021.

[20] A. Waqas, M. J. U. Rehman, H. Dilpazir, M. F. Sohail, and N. Subhani, "A method to reduce route discovery cost of UAV ad hoc network," *Int. J. Distrib. Sensor Netw.*, vol. 2023, pp. 1–10, May 2023.

[21] R. Jarray, M. Al-Dhaifallah, H. Rezk, and S. Bouallègue, "Parallel cooperative coevolutionary grey wolf optimizer for path planning problem of unmanned aerial vehicles," *Sensors*, vol. 22, no. 5, p. 1826, Feb. 2022.

[22] L. Yao, P. Yuan, C.-Y. Tsai, T. Zhang, Y. Lu, and S. Ding, "ESO: An enhanced snake optimizer for real-world engineering problems," *Expert Syst. Appl.*, vol. 230, Nov. 2023, Art. no. 120594.

[23] J. Wang, B. Zhang, and L. Shu, "Research on non-intrusive load recognition method based on improved equilibrium optimizer and SVM model," *Electronics*, vol. 12, no. 14, p. 3138, Jul. 2023.